# Microwave absorption properties of a double-layer absorber based on nanocomposite $BaFe_{12}O_{19}/\alpha$-Fe and nanocrystalline $\alpha$-Fe microfibers*

Shen Xiang-Qian(沈湘黔)†, Liu Hong-Bo(刘洪波), Wang Zhou(王 舟), Qian Xin-Ye(钱昕晔), Jing Mao-Xiang(景茂祥), and Yang Xin-Chun(杨新春)

*Institute for Advanced Materials, Jiangsu University, Zhenjiang* 212013, *China*

(Received 13 December 2013; revised manuscript received 6 January 2014; published online 28 May 2014)

The nanocomposite $BaFe_{12}O_{19}/\alpha$-Fe and nanocrystalline $\alpha$-Fe microfibers with diameters of 1–5 μm, high aspect ratios and large specific areas are prepared by the citrate gel transformation and reduction process. The nanocomposite $BaFe_{12}O_{19}/\alpha$-Fe microfibers show some exchange–coupling interactions largely arising from the magnetization hard ($BaFe_{12}O_{19}$) and soft ($\alpha$-Fe) nanoparticles. For the microwave absorptions, the double-layer structures consisting of the nanocomposite $BaFe_{12}O_{19}/\alpha$-Fe and $\alpha$-Fe microfibers each exhibit a wide band and strong absorption behavior. When the nanocomposite $BaFe_{12}O_{19}/\alpha$-Fe microfibers are used as a matching layer of 2.3 mm in thickness and $\alpha$-Fe microfibers as an absorbing layer of 1.2 mm in thickness, the optimal reflection loss (RL) achieves −47 dB at 15.6 GHz, the absorption bandwidth is about 12.7 GHz ranging from 5.3 to 18 GHz, exceeding −20 dB, which covers 72.5% *C*-band (4.2–8.2 GHz) and whole *X*-band (8.2–12.4 GHz) and $K_u$-band (12.4–18 GHz). The enhanced absorption properties of these double-layer absorbers are mainly ascribed to the improvement in impedance matching ability and microwave multi-reflection largely resulting from the dipolar polarization, interfacial polarization, exchange–coupling interaction, and small size effect.

**Keywords:** $BaFe_{12}O_{19}$, $\alpha$-Fe, microfiber, double-layer absorber

**PACS:** 81.07.Bc, 75.50.–y, 73.21.AC **DOI:** 10.1088/1674-1056/23/7/078101

## 1. Introduction

As a special kind of environment pollution, the electromagnetic interference (EMI) has attracted much attention due to the increasing uses of local computer networks, mobile phones, and high frequency electronic devices. In order to solve the EMI problem, various microwave absorption materials have been investigated and widely used.[1–7] Liu *et al.* prepared $\alpha$-Fe/Z-type Ba-ferrite composites with strong microwave absorption in a 6.1–13.6 GHz range (RL < −10 dB).[8] Han *et al.* synthesized the carbonyl iron/Ni-Zn ferrite composite and achieved a strong attenuation of microwaves in 1–4 GHz range (RL < −10 dB).[9] Yang *et al.* reported on microwave absorption properties of the nanocomposite $BaFe_{12}O_{19}/\alpha$-Fe microfibers.[10] Ren *et al.* investigated the nanocomposites consisting of $SiO_2$@$Fe_3O_4$ nanorods, $Fe_3O_4$@Fe nanopariticles and graphene and their efficient microwave absorption performances.[11,12] However, these materials are usually designed as a single-layer structure and hard to simultaneously meet the requirements for low weight and strong absorption in a wide frequency range.

Recently, multi- and double-layer structures have emerged as a novel strategy to solve the EMI problem.[13–15] Due to appropriate preparative process the double-layer structure is particularly attractive, and it is often constructed by two different materials with excellent impedance matching ability and can obtain a high attenuation for the incident electromagnetic wave.[16] Lee *et al.*[17] designed the absorbing structures composed of multi-walled carbon nanotubes filled glass and epoxy plain-weave. The results showed that the RL less than −10 dB obtained in a frequency range of 8.9–12.0 GHz with a total thickness value of 2.4 mm. Duan *et al.*[18] have studied the microwave absorption behavior of the double-layer absorber based on $\alpha$-MgO and carbon black, and found that the double-layer structure could provide an excellent absorption property with a wide bandwidth of 9.3–18 GHz (RL < −10 dB) and a thickness value of 5 mm.

Metallic magnetic materials are usually used to shield electromagnetic waves as their permeability can remain high in a gigahertz range. However, the reflecting waves from metals may cause imaginary degradation effects. Hexaferrites have been well known as absorbing materials due to the strong magnetic loss.[19–21] However, up to now, there have been few reports about double-layer absorbers based on the hexaferrite composite and magnetic metals. In the present study,

*Project supported by the National Natural Science Foundation of China (Grant Nos. 51274106 and 51202091), the Natural Science Foundation of Jiangsu Provincial Higher Education, China (Grant No. 12KJA430001), the Science and Technology Support Program of Jiangsu Province, China (Grant Nos. BE2012143 and BE2013071), the Jiangsu Provincial Postgraduate Cultivation and Innovation Project, China (Grant No. CXZZ13_0662), and the Priority Academic Program Development of Jiangsu Higher Education Institutions, China (Grant No. 1033000003).

†Corresponding author. E-mail: shenxq@ujs.edu.cn

© 2014 Chinese Physical Society and IOP Publishing Ltd 

we choose the nanocomposite $BaFe_{12}O_{19}/\alpha$-Fe microfibers and nanocrystalline metallic $\alpha$-Fe microfibers as absorbents and designed double-layer absorbers. These pure and binary phase microfibers are all prepared by the citrate gel method with a porous structure, large specific area and strong shape anisotropy.

## 2. Experimental procedure

The nanocomposite $BaFe_{12}O_{19}/\alpha$-Fe microfibers and nanocrystalline $\alpha$-Fe microfibers were prepared by the citrate gel transformation and selective reduction process, which has been described in detail in our previous studies.[22,23] The X-ray diffraction (XRD) patterns of the as-prepared microfibers were obtained by a Rigaku D/Mmax2500PC diffractometer with Cu K$\alpha$ radiation, and the diffraction data were recorded from 20° to 80°. Morphologies of microfibers were investigated by field emission scanning electron microscopy (FE-SEM, JSM-7001F). Magnetic measurements were performed at room temperature using a vibrating sample magnetometer (VSM, HH-15) with a maximum applied field of 1194 kA/m (15 kOe).

In order to determine the microwave absorbing properties of these microfibers, we investigated the electromagnetic parameters of the paraffin wax-based composite containing 67% mass fraction of $BaFe_{12}O_{19}/\alpha$-Fe microfibers as Specimen 1 (S1) and the paraffin wax-based composite containing 67% mass fraction of $\alpha$-Fe microfibers as Specimen 2 (S2) in a frequency range of 2–18 GHz. Subsequently, the paraffin wax-based microfibers composites were machined into a toroidal shape with an outer diameter of 7.0 mm and an inner diameter of 3.04 mm for microwave measurement. The electromagnetic (EM) parameters ($\varepsilon'$ for the real part of permittivity, $\varepsilon''$ for the imaginary part of permittivity, $\mu'$ for the real part of permeability, and $\mu''$ for the imaginary part of permeability) of specimen were measured using Hewlett Packard 8722ES network analyzer at frequencies in a range of 2–18 GHz.

According to the transmission line theory, for a single-layer absorber with different thickness values backed a metal plate, the reflection loss (RL) can be calculated using the EM parameters by means of the following expressions:[6,8]

$$Z_{\text{in}} = Z_0\left(\frac{\mu_{\text{r}}}{\varepsilon_{\text{r}}}\right)^{1/2}\tanh\left[\text{j}\left(\frac{2\pi df}{c}\right)(\mu_{\text{r}}\varepsilon_{\text{r}})^{1/2}\right], \quad (1)$$

$$\text{RL} = 20\log|(Z_{\text{in}} - Z_0)/(Z_{\text{in}} + Z_0)|, \quad (2)$$

where $c$ is the light velocity, $f$ is the frequency of the microwave, $d$ is the absorber thickness, $\varepsilon_{\text{r}}$ is the complex permittivity ($\varepsilon'$–j$\varepsilon''$), $\mu_{\text{r}}$ is the complex permeability ($\mu'$–j$\mu''$), $Z_0$ is the air impedance, and $Z_{\text{in}}$ is the input impedance of the absorber.

For a multi-layer microwave absorber, its microwave absorption performance can be calculated based on the following equation:[14]

$$_n\frac{Z_{\text{in}(n-1)} + \eta_n\tanh(\gamma_n d_n)}{\eta_n + Z_{\text{in}(n-1)}\tanh(\gamma_n d_n)}, \quad (3)$$

where $\eta_n$ and $\gamma_n$, respectively, are the characteristic impedance and the propagation constant of the nth layer, and they are given as

$$\eta_n = \eta_0\sqrt{\frac{\mu_{rn}}{\varepsilon_{rn}}}, \quad (4)$$

$$\gamma_n = \text{j}\omega(\varepsilon_0\mu_0\varepsilon_n\mu_n)^{1/2} = \frac{\text{j}2\pi}{\lambda}\sqrt{\mu_n\varepsilon_n}, \quad (5)$$

where $Z_n$ is the input impedance of the $n$-th layer; and $\varepsilon_n$ and $\mu_n$ are the complex relative permittivity and permeability of the $n$-th layer, respectively. Using Eqs. (1)–(5), the overall reflection loss for the multi-layer absorber is given by

$$\text{RL} = 20\log|(Z_{\text{in}}(n) - Z_0)/(Z_{\text{in}}(n) + Z_0)|. \quad (6)$$

## 3. Results and discussion

### 3.1. Characteristics of $BaFe_{12}O_{19}/\alpha$-Fe and $\alpha$-Fe microfibers

Figure 1 shows SEM morphologies and XRD patterns of nanocomposite $BaFe_{12}O_{19}/\alpha$-Fe and nanocrystalline $\alpha$-Fe microfibers. From Figs. 1(a)–1(c), it can be seen that these microfibers possess high aspect ratios and uniform diameters ranging from 1 to 5 μm. In the obtained microfibers, the porous structure on a nanoscale can be observed. This structure will benefit the attenuation of electromagnetic waves due to their high specific surface area and strong interface polarization. Figure 1(d) shows the XRD patterns of $BaFe_{12}O_{19}/\alpha$-Fe and $\alpha$-Fe microfibers, indicating that all the diffraction peaks belong to the $BaFe_{12}O_{19}$ (JCPDS 27-1029) and $\alpha$-Fe (JCPDS 06-0696) phases. The average values of grain size ($D$) are estimated using the Debye–Scherrer equation to be 44 nm for the $\alpha$-Fe in $\alpha$-Fe microfibers, 29 nm of $\alpha$-Fe, and 39 nm for $BaFe_{12}O_{19}$ in the composite microfibers, respectively. This proves that these pure and binary microfibers are fabricated from nanoparticles.

The hysteresis loops of $BaFe_{12}O_{19}/\alpha$-Fe and $\alpha$-Fe microfibers are shown in Fig. 2. From Fig. 2, it can be seen that the $BaFe_{12}O_{19}/\alpha$-Fe microfibers each possess a saturation magnetization (73.9 $\text{A}\cdot\text{m}^2\cdot\text{kg}^{-1}$) combined with a high coercivity (81.6 kA/m), implying that the magnetization hard ($BaFe_{12}O_{19}$) and soft ($\alpha$-Fe) phases are well exchange coupled.[24,25] While the pure $\alpha$-Fe microfibers exhibit a typical soft behavior.

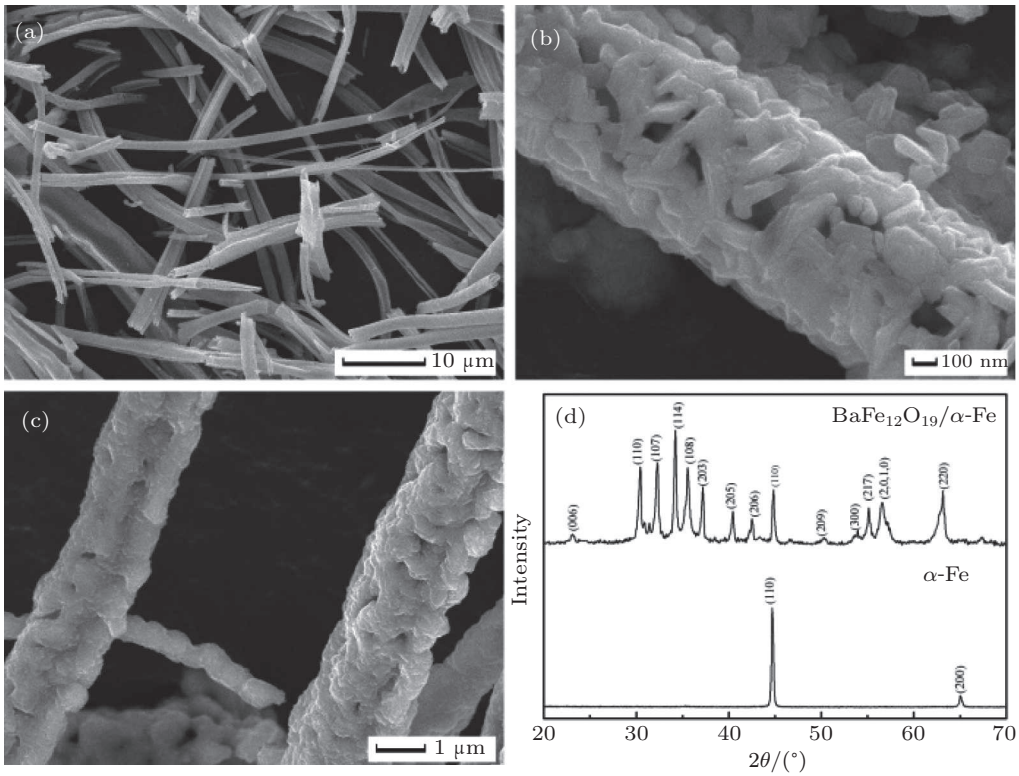



**Fig. 1.** SEM morphologies of (a), (b) nanocomposite $BaFe_{12}O_{19}/\alpha$-Fe microfibers, (c) $\alpha$-Fe microfibers, and (d) XRD patterns of the nanocomposite $BaFe_{12}O_{19}/\alpha$-Fe and $\alpha$-Fe microfibers.

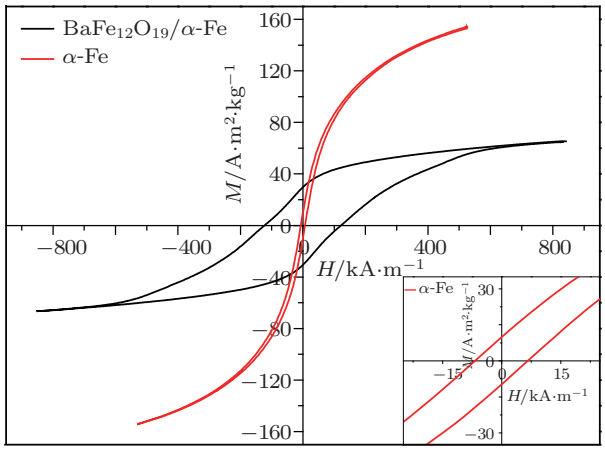



**Fig. 2.** (color online) Magnetic hysteresis loops at room temperature of nanocomposite $BaFe_{12}O_{19}/\alpha$-Fe and $\alpha$-Fe microfibers. The inset shows the low coercivity of $\alpha$-Fe microfibers.

### 3.2. Characteristics of electromagnetic parameters

Usually, the microwave absorption behaviors of materials depend on the values of complex relative permittivity ($\varepsilon_r = \varepsilon' - j\varepsilon''$) and permeability ($\mu_r = \mu' - j\mu''$). Figures 3(a) and 3(b) represent the frequency dependences of the complex permittivity ($\varepsilon_r$) and permeability ($\mu_r$) for nanocomposite $BaFe_{12}O_{19}/\alpha$-Fe microfibers. From Fig. 3(a), it can be observed that the real part ($\varepsilon'$) of $BaFe_{12}O_{19}/\alpha$-Fe decreases gradually with the increase of frequency. While the imaginary part ($\varepsilon''$) keeps a slowly decreasing tendency except for a broad peak in a frequency range of 12–16 GHz. This phenomenon can be attributed to the dipolar polarization and interface polarization.[26–28] For the complex permeability ($\mu_r$) of $BaFe_{12}O_{19}/\alpha$-Fe microfiber as shown in Fig. 3(b), the real part $\mu'$ remains almost a constant in the measured frequency range, whereas the $\mu''$ maintains an increasing tendency in the measured frequency range except for a broad peak at 14–18 GHz. There is no dramatic decrease in the high frequency range, implying that the eddy current effects resulting from the metallic $\alpha$-Fe are effectively suppressed by the semiconducting $BaFe_{12}O_{19}$ grains in the composite microfibers. In addition, the sufficient exchange coupling interaction between the magnetization soft ($\alpha$-Fe) and hard ($BaFe_{12}O_{19}$) particles arising from small size effect will also enhance the magnetic loss.

Figures 3(c) and 3(d) show the permittivity ($\varepsilon_r$) and permeability ($\mu_r$) for the nanocrystalline $\alpha$-Fe microfibers respectively. It can been seen that the real part $\varepsilon'$ exhibits a decreasing tendency with the increase of frequency, while the imaginary part $\varepsilon''$ has an increasing tendency in a range of 2–5 GHz and then decreases in a range from 5 to 18 GHz. This phenomenon may be related to the damping of the electrical dipole vibrations and interface polarization. From Fig. 3(d), the $\mu'$ value shows a decreasing tendency in the measured frequency range with two broad peaks appearing around 8 and 13 GHz. While the imaginary part $\mu''$ exhibits a decreasing tendency in the whole frequency range except for some small

peaks. These observed peaks can be attributed mainly to the natural ferromagnetic resonance and domain wall displacement arising from the interface effect, small size effect and spin wave excitations.[29] The values of complex permittivity and permeability of these microfibers are higher and more stable than those reported for pure hexaferrites[30] and metal powders,[31] which can lead to a wider microwave absorption bandwidth.

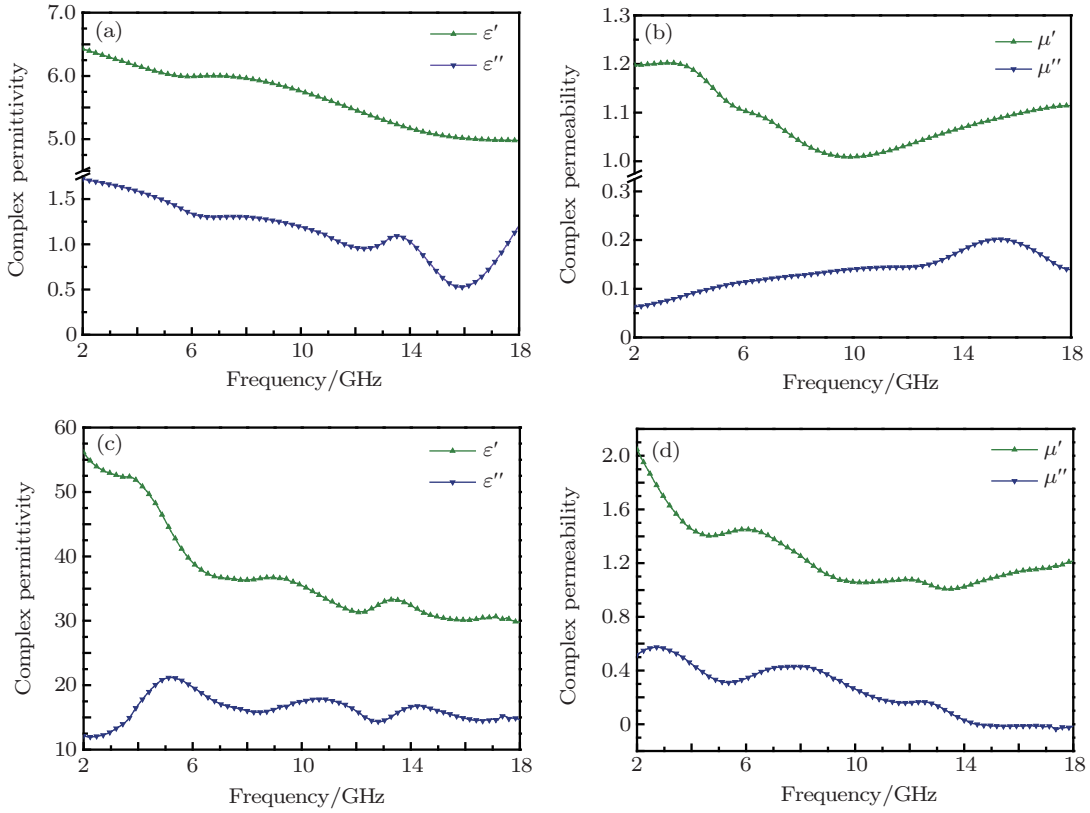



**Fig. 3.** (color online) Curves of complex relative permittivity and permeability versus frequency of (a), (b) $BaFe_{12}O_{19}/\alpha$-Fe microfibers and (c), (d) $\alpha$-Fe microfibers.

### 3.3. Microwave absorption of single-layer and double-layer absorbers

In general, the RL value −20 dB corresponds to about 99% attenuation of *EM* wave energy and can be considered as an effective absorption in practical applications. The values of RL in a frequency range of 2–18 GHz for single-layer structures of nanocomposite $BaFe_{12}O_{19}/\alpha$-Fe and nanocrystalline $\alpha$-Fe microfibers with various thickness values are shown in Fig. 4. It can be seen that the optimal RL value of $BaFe_{12}O_{19}/\alpha$-Fe microfiber reaches −26.8 dB at 18 GHz, and the absorption bandwidth with RL value less then −20 dB is about 3.8 GHz.[10] The frequency of the minimum RL is shifted toward a lower frequency range with the increase of thickness value. Compared with $BaFe_{12}O_{19}/\alpha$-Fe microfibers, the nanocrystalline $\alpha$-Fe microfibers show a low microwave absorption. When the thickness value is 2.0 mm, the minimum RL value reaches about −15.1 dB at 4 GHz. When the thickness value increases to 3.5 mm, the minimum RL value is shifted toward lower frequencies and achieves about −24.8 dB at 2 GHz.

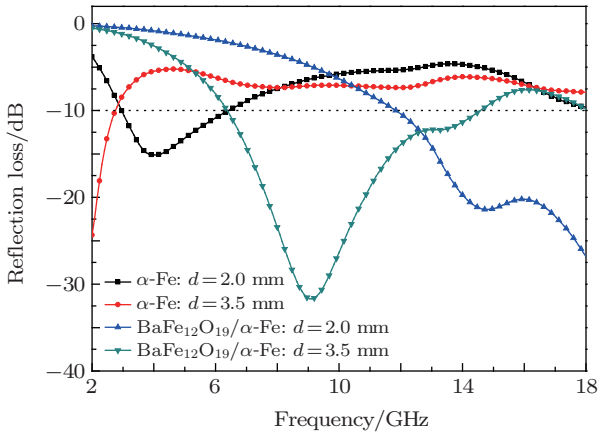



**Fig. 4.** (color online) Curves of reflection loss versus frequency for the single-layer microwave absorber with different thickness values.

Figure 5(a) shows the RL values of the double-layer structure composed of $\alpha$-Fe microfibers as the matching layer and $BaFe_{12}O_{19}/\alpha$-Fe microfibers as the absorbing layer, with total thickness value being 2 mm, and figure 5(b) displays

the RL values of the double-layer structure composed of $BaFe_{12}O_{19}/\alpha$-Fe microfibers as the matching layer and $\alpha$-Fe microfibers as the absorbing layer, with total thickness value being 2 mm. From Fig. 5(a), it can be seen that when the thickness value of $\alpha$-Fe microfiber matching layer is 0.6 mm and that of $BaFe_1a_2O_{19}/\alpha$-Fe microfiber absorbing layer is 1.4 mm, the double-layer structure achieves a minimum RL value of $-22.9$ dB at 6.8 GHz, with a narrow bandwidth about 1.5 GHz (RL $< -20$ dB). Whereas, when $\alpha$-Fe and $BaFe_{12}O_{19}/\alpha$-Fe microfibers are used as the matching layer and absorbing layer respectively (Fig. 5(b)), the minimum RL value achieves $-35$ dB at 14.5 GHz, and the absorption bandwidth can reach 5.8 GHz ranging from 12.2 to 18 GHz where the RL value exceeds $-20$ dB. Especially, the optimal RL value of $-39$ dB is obtained at 13.8 GHz with the thickness value of matching layer being 0.9 mm, while the absorption bandwidth (RL $< -20$ dB) covers the 38% $X$-band (8.2–12.4 GHz) and 71.4% $K_u$-band (12.4–18.0 GHz). This variation trend can be explained based on the attenuation properties of the magnetic materials. With a lower dielectric constant of $BaFe_{12}O_{19}/\alpha$-Fe microfibers, the impedance of matching layer is close to $Z_0$ and the microwave can enter into the absorber as much as possible. Simultaneously, the incident microwave in the absorbers can be almost entirely attenuated rapidly as the $\alpha$-Fe microfiber layer possesses a higher dielectric and magnetic loss. Therefore, the multi-reflection and loss of microwaves improve the absorption property of the double-layer structure when they are combined with an optimal combination.

Figure 6 shows the RL value curves of the double-layer absorbers composed of $BaFe_{12}O_{19}/\alpha$-Fe as the matching layer and $\alpha$-Fe microfibers as the absorbing layer, with total thickness being 3.5 mm. It can be observed that the bandwidth exceeding $-20$ dB improves significantly. When the matching layer is 2.3mm thick and absorber layer is 1.2 mm thick, the optimal RL value of $-47$ dB is obtained at 15.6 GHz, with a broad absorption bandwidth RL value being less than $-20$ dB in the bandwidth 12.7 GHz ranging from 5.3 to 18 GHz, which covers the 72.5% $C$-band (4.2–8.2 GHz), the whole $X$-band (8.2–12.4 GHz) and $K_u$-band (12.4–18 GHz). It is interesting to note that the minimum RL decreases as the thickness value of matching layer increases. The possible reason is that the thickness value can change the impedance matching between the materials and the free space, or between the absorbing layer and the matching layer, which can lead to a strong wave reflection on the absorber surface and act against incidence and absorption of the transmission microwave in the absorber.

Table 1 shows the comparison of microwave absorption characteristic between some recently reported double-layer structures. Compared with the double-layer structures reported in the references, the double-layer structure based on the binary $BaFe_{12}O_{19}/\alpha$-Fe and pure $\alpha$-Fe microfibers exhibits a strong microwave absorption in a wide frequency range. Thus, these double-layer structures consisting of $BaFe_{12}O_{19}/\alpha$-Fe and $\alpha$-Fe microfibers can be used as a high performance absorber.

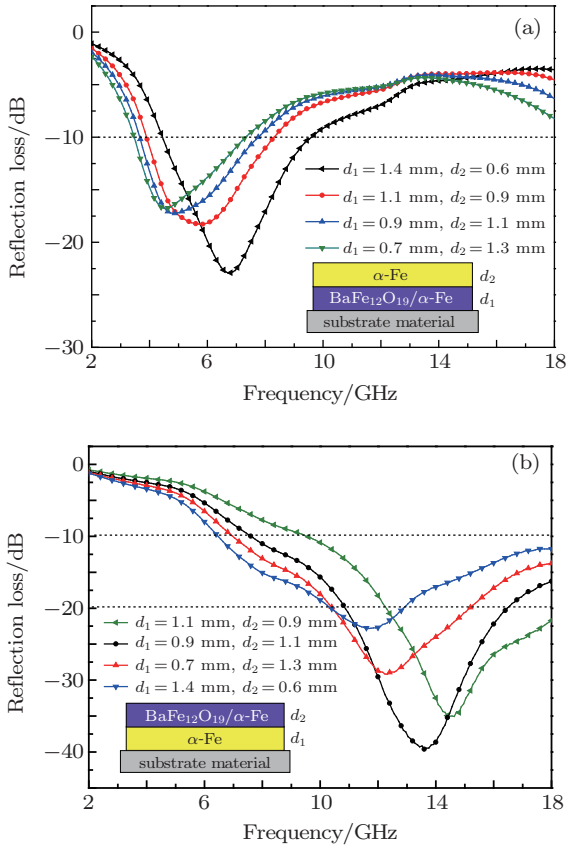



**Fig. 5.** (color online) Curves of reflection loss versus frequency of the double-layer microwave absorber with total thickness of 2 mm based on: (a) $\alpha$-Fe microfibers (matching layer) and nanocomposite $BaFe_{12}O_{19}/\alpha$-Fe microfibers (absorbing layer), (b) nanocomposite $BaFe_{12}O_{19}/\alpha$-Fe microfibers (matching layer) and $\alpha$-Fe microfibers (absorbing layer).

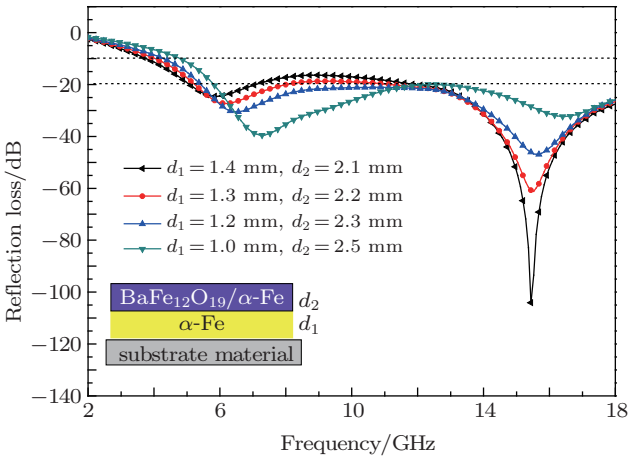



**Fig. 6.** (color online) Curves of reflection loss versus frequency of the double-layer microwave absorber based on nanocomposite $BaFe_{12}O_{19}/\alpha$-Fe microfibers (matching layer) and $\alpha$-Fe microfibers ( absorbing layer) with a total thickness of 3.5 mm.

**Table 1.** Comparison of microwave absorption property between some recent reported double-layer microwave absorbers.

| Double-layer absorbers | Bandwidth/GHz | $d$/mm | MRL/dB | $f$/GHz | Ref. |
|---|---|---|---|---|---|
| Based on $BaTiO_3$ and carbonyl iron | 5.2–6.3 | 2.2 | –53 | 5.7 | [10] |
| Based on carbonyl iron and carbon black | 4.9 –5.8 | 4 | –23.8 | 5.3 | [13] |
| Based on carbon nanotubes and epoxy weave | 9.2–10.4 | 3.27 | –30 | 9.5 | [14] |
| Based on manganese oxide and carbon black | 13.5–14.8 | 4 | –25.2 | 14.3 | [15] |
| Based on nanocomposite $BaFe_{12}O_{19}/\alpha$-Fe and $\alpha$-Fe microfibers | 5.3–18 | 3.5 | –47 | 15.6 | This work |

Note: RL is less than −20 dB; $d$ denotes the total thickness, MRL the minimum RL value, and $f$ the frequency at minimum RL value.

## 4. Conclusions

The single-layer and double-layer microwave absorbers with various thickness values are designed based on the nanocomposite $BaFe_{12}O_{19}/\alpha$-Fe microfibers and nanocrystalline $\alpha$-Fe microfibers. The double-layer structure microwave absorbers exhibit stronger absorption properties in a wider frequency range than the single-layer absorbers. The absorption properties are mainly influenced by the thickness value of each layer and the total thickness value of the absorber. When the nanocomposite $BaFe_{12}O_{19}/\alpha$-Fe microfibers are used as the matching layer, strong microwave absorption can be obtained in a wide frequency range. When the thickness value of the matching layer is 2.3 mm ($BaFe_{12}O_{19}/\alpha$-Fe) and that of the absorbing layer is 1.2 mm ($\alpha$-Fe), the absorption bandwidth with an RL value less than −20 dB is 12.7 GHz ranging from 5.3 GHz to 18 GHz, covering 72.5% of the $C$-band (4.2–8.2 GHz) and the whole $X$-band (8.2–12.4 GHz), and $K_u$-band (12.4–18 GHz). These double-layer absorbers are promising advanced microwave absorbers.

## References


[1] Wang Q S, Lei Z Y, Chen Y J, Ouyang Q Y, Gao P, Qi L H, Zhu C L and Zhang J Z 2013 *J. Mater. Chem. A* **1** 11795

[2] Fannin P C, Marin C N, Malaescu I, Stefu N, Vlazan P, Novaconi S, Sfirloaga P, Popescu S and Couper C 2011 *Mater. Des.* **32** 1600

[3] Pan X F, Shen H G, Qiu J X and Gu M Y 2007 *Mater. Chem. Phys.* **101** 505

[4] Zhou P H and Deng L J 2009 *IEEE Trans. Magn.* **45** 663

[5] Yu H L, Wang T S, Wen B, Lu M M, Xu Z, Zhu C L, Chen Y J, Xue X Y, Sun C W and Cao M S 2012 *J. Mater. Chem.* **22** 21679

[6] Abbas S M, Dixit A K, Chatterjee R and Goel T C 2007 *J. Magn. Magn. Mater.* **309** 20

[7] Han M G, Ou Y, Liang D F and Deng L J 2009 *Chin. Phys. B* **18** 1261

[8] Liu J R, Itoh M and Machida K 2006 *Appl. Phys. Lett.* **88** 062503

[9] Han R, Gong L Q, Wang T, Qiao L and Li F S 2012 *Mater. Chem. Phys.* **131** 555

[10] Yang X C, Liu R J, Shen X Q, Song F Z, Jing M X and Meng X F 2013 *Chin. Phys. B* **22** 058101

[11] Ren Y L, Zhu C L, Zhang S, Li C Y, Chen Y J, Gao P, Yang P P and Ouyang Q Y 2013 *Nanoscale* **5** 12296

[12] Ren Y L, Wu H Y, Lu M M, Chen Y J, Zhu C L, Gao P, Cao M S, Li C Y and Ouyang Q Y 2012 *ACS Appl. Mater. Interfaces* **4** 6436

[13] Chen L Y, Duan Y P, Liu L D, Guo J B and Liu S H 2011 *Mater. Des.* **32** 570

[14] Qing Y C, Zhou W C, Luo F and Zhu D M 2011 *J. Magn. Magn. Mater.* **323** 600

[15] Wang M, Duan Y P, Liu S H, Li X G and Ji Z J 2009 *J. Magn. Magn. Mater.* **321** 3442

[16] Wei C Y, Shen X Q and Song F Z 2012 *Chin. Phys. B* **21** 028101

[17] Lee S E, Kang J H and Kim C G 2006 *Compos. Strcut.* **76** 397

[18] Duan Y P, Yang Y, He M, Liu S H, Cui X D and Chen H F 2008 *J. Phys. D: Appl. Phys.* **41** 125403

[19] He J H, Wang W, Wang A M and Guan J G 2012 *J. Magn. Magn. Mater.* **324** 2902

[20] Ghasemi A, Liu X X and Morisako A 2007 *J. Magn. Magn. Mater.* **316** 105

[21] Ghasemi A, Hossienpour A, Morisako A, Liu X X and Ashrafizadeh A 2008 *Mater. Des.* **29** 112

[22] Yang X C, Liu R J, Shen X Q and Song F Z 2012 *J. Sol–Gel Sci. Technol.* **63** 8

[23] Song F Z, Shen X Q, Xiang J and Zhu Y W 2010 *J. Alloy. Compd.* **507** 297

[24] Maeda T, Sugimoto S, Kagotani T, Tezuka N and Inomata K 2004 *J. Magn. Magn. Mater.* **281** 195

[25] Cui B Z, Han K, Garmestani H, Su J H, Schneider-Muntau J H and Liu J P 2005 *Acta Mater.* **53** 4155

[26] Zhang L Y and Li Z W 2009 *J. Alloys. Compd.* **469** 422

[27] Feng Y B, Qiu T, Shen C Y and Li X Y 2006 *IEEE Trans. Magn.* **42** 363

[28] Tong G X, Wu W H, Hua Q, Miao Y Q, Guan J G and Qian H S 2011 *J. Alloy. Compd.* **509** 451

[29] Ruan S P, Xu B K, Suo H, Wu F Q, Xiang S Q and Zhao M Y 2000 *J. Magn. Magn. Mater.* **212** 175

[30] Ohlan A, Singh K, Chandra A and Dhawan S K 2008 *Appl. Phys. Lett.* **93** 0531141

[31] Han R, Qiao L, Wang T and Li F S 2011 *J. Alloy. Compd.* **509** 2734